Stability of shortest paths in complex networks with random edge weights

Jae Dong Noh and Heiko Rieger

Theoretische Physik, Universität des Saarlandes, 66041 Saarbrücken, Germany

(Received 22 August 2002; published 19 December 2002)

We study shortest paths and spanning trees of complex networks with random edge weights. Edges which do not belong to the spanning tree are inactive in a transport process within the network. The introduction of quenched disorder modifies the spanning tree such that some edges are activated and the network diameter is increased. With analytic random-walk mappings and numerical analysis, we find that the spanning tree is unstable to the introduction of disorder and displays a phase-transitionlike behavior at zero disorder strength $\varepsilon = 0$. In the infinite network-size limit ($N \to \infty$), we obtain a continuous transition with the density of activated edges Φ growing like $\Phi \sim \varepsilon^1$ and with the diameter-expansion coefficient Υ growing like $\Upsilon \sim \varepsilon^2$ in the regular network, and first-order transitions with discontinuous jumps in Φ and Υ at $\epsilon = 0$ for the small-world (SW) network and the Barabási-Albert scale-free (SF) network. The asymptotic scaling behavior sets in when $N \gg N_c$, where the crossover size scales as $N_c \sim \varepsilon^{-2}$ for the regular network, $N_c \sim \exp(\alpha \varepsilon^{-2})$ for the SW network, and $N_c \sim \exp(\alpha |\ln \varepsilon| \varepsilon^{-2})$ for the SF network. In a transient regime with $N \ll N_c$, there is an infinite-order transition with $\Phi \sim \Upsilon \sim \exp[-\alpha/(\varepsilon^2 \ln N)]$ for the SW network and $\sim \exp[-\alpha/(\varepsilon^2 \ln N/\ln \ln N)]$ for the SF network. It shows that the transport pattern is practically most stable in the SF network.

PACS number(s): 89.75.−k, 05.10.−a, 75.10.Nr, 05.40.Fb

I. INTRODUCTION

A network is a new paradigm to study complex systems in many disciplines in science [1,2]. A complex system consists of a large number of interacting units and the nature of the interaction determines equilibrium and dynamical properties of the system. Frequently, the simplifying assumption is made that the units are arranged to form a simple pattern like a regular lattice or to interact with all others as in a mean-field theory. Recent studies, however, have revealed that the structure of complex systems is much richer [1–3]. In general this structure is captured by a network which consists of vertices representing the units and edges connecting interacting vertex pairs.

Complex networks exhibit so-called small-world phenomena: vertices are highly clustered and the average separation between vertices grows slowly with the total number of vertices. Watts and Strogatz [3] introduced a small-world (SW) network as a model for these phenomena. It is obtained from a regular lattice with edges randomly rewired with probability p_r. Later it was found that some complex networks have a power-law distribution $P_{deg}(z) \sim z^{-\gamma}$ of the degree z. The degree of a vertex is the number edges incident upon it. The class of networks with a power-law degree distribution is called the class of scale-free (SF) networks and is found in many areas including physics, computer science, biology, sociology, etc (we refer readers to Ref. [2] for examples). The Barabási-Albert model [4] generates a SF network ($\gamma = 3$) *growing* via a *preferential attachment* rule [5]. Initially one starts with Z_0 vertices and introduces a new vertex at each step (growing). It is then attached to Z existing vertices, which are selected with probability *linearly* proportional to their degree (preferential attachment).

The discovery of these classes of networks triggered extensive research. Order-disorder phase transitions [6–8] and nonequilibrium phase transitions [9] have been studied. Interestingly, the critical behavior is described well by mean-field theories and strongly depends on the degree distribution [7]. Stability of complex networks has also been studied against a strong disorder such as a vertex dilution [10–12]. When the fraction of diluted vertices increases, a network may disintegrate into finite clusters undergoing a percolation-type transition. In this paper, we study the effect of weak disorder on the transport properties of networks.

The *shortest path* plays an important role for the transport within a network [13,14]. A *path* denotes a sequence of vertices, successive pairs of which are connected via edges. In general there exist many paths connecting two given vertices. The shortest path is the one with minimum path length among all the paths. The minimum path length is called a *separation* between the two vertices. Suppose one needs to send, e.g., a data packet from one computer to the other through the Internet. The shortest path provides an optimal path way since one would achieve a fastest transfer and save system resources. The shortest path is also important in studying an internal structure of a network [15]. The separation can be used as a measure of intimacy between vertices. The number of shortest paths that pass through a vertex is called the "betweenness" or "load" [15,13,14,16]. It reflects the importance of a vertex in mutual relationship or in transport. The load follows universal power-law distributions in scale-free networks [13,14,16].

Consider shortest paths from a vertex s, called the *source*, to all other vertices in a network. In an unweighted network the length of a path is just the number of edges that it contains and shortest paths can simply be found using the "breadth-first search algorithm" [17]. A subnetwork consisting of all the shortest paths from s is the *spanning tree* $\mathbf{T}_s$, which characterizes the optimal transport pattern. Figure 1 shows an example of a network and its spanning tree. It is convenient to represent the spanning tree by a diagram in which vertices are arranged hierarchically in the ascending order of their separation from the source. Then, the shortest path to each vertex is given by a directed path on $\mathbf{T}_s$. In
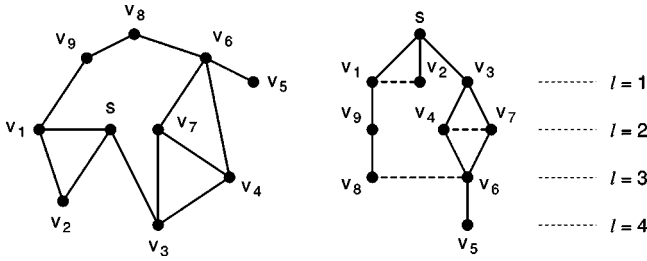
FIG. 1. A network (left) and its spanning tree (right) $\mathbf{T}_s$. Vertices in $\mathbf{T}_s$ are arranged in the hierarchical order of the separation l. The vertex v_6, and hence v_5, has twofold degenerate shortest paths, so $\mathbf{T}_s$ contains a loop. Dashed lines represent edges which do not belong to $\mathbf{T}_s$.

general, the spanning tree does not have a tree structure. If there are degenerate shortest paths, $\mathbf{T}_s$ contains a loop. Some edges do not belong to $\mathbf{T}_s$. They do not contribute to any flow from or to s.

It has been assumed that all edges are equivalent having the same cost. However, a real network would be described better with weighted edges. A weight of an edge may represent an access cost, a physical length, or an intimacy between vertices [15,18]. For example, edges between scientists in scientific collaboration networks may have weights which depends on the number of coauthored papers [15]. In a weighted network, the path with the minimum number of edges is not necessarily an optimal one. In this work, we study disordered networks with randomly weighted edges and investigate the effect of the disorder on the transport pattern. The regular network, the SW network [3], and the Barabási-Albert SF network [4] are considered. This paper is organized as follows: In Sec. II, we define the shortest path and the spanning tree in the disordered network. The disorder modifies the shape of the spanning tree. The response is described for the regular and SW networks in Sec. III and for the SF network in Sec. IV. We conclude in Sec. V.

II. SHORTEST PATHS AND THE SPANNING TREE OF DISORDERED NETWORKS

Consider a disordered undirected network. An edge e between two vertices u and v will be denoted as $e=[u;v]=[v;u]$. To each edge e a non-negative weight $c(e)$ is assigned which is called the *edge cost* of e. Here we neglect all system-dependent details and assume that

$$c(e)=1+\eta(e),\qquad(1)$$

where $\eta(e)$'s are random variables distributed independently with distribution $\mathcal{F}(\eta)$ ($\eta(e)>-1$).

In a disordered network, a *minimum-cost path* plays the role of the shortest path in a pure ($\eta=0$) network. For given vertices u and v, the minimum-cost path is given by the one with minimum *path cost*. The path cost is defined as the sum of all edge costs in the path. Without disorder [$\eta(e)=0$ for all e], the path cost is equivalent to the path length and the minimum-cost path is the same as the shortest path. Hereafter, the minimum-cost path will be called the shortest path,

and the minimum cost is denoted as a *distance*. The path length of the shortest path is called the *separation* of the two vertices connected by it.

The spanning tree $\mathbf{T}_s$ of a disordered network can be found using the "Dijkstra algorithm" [17]: Divide all vertices into two sets, S and its complement $\bar{S}$. Initially $S=\{s\}$ and the source is assigned to a distance label $d(s)=0$ and a separation label $l(s)=0$. At each iteration, one selects an optimal edge $e^*=[u^*;v^*]$ that has a minimum value of $d(u)+c([u;v])$ among all edges $e=[u;v]$ with $u\in S$ and $v\in\bar{S}$. Then, the vertex v^* gets the labels $d(v^*)=d(u^*)+c([u^*;v^*])$ and $l(v^*)=l(u^*)+1$ and a predecessor label $\mathrm{pred}(v^*)=u^*$, and is shifted from $\bar{S}$ to S. The iteration terminates when the set $\bar{S}$ is empty. The shortest path to each vertex is then found by tracing the predecessor iteratively back to s. The distance and separation from s to each vertex v are given by $d(v)$ and $l(v)$, respectively. The average separation $D_s=[1/(N-1)]\Sigma_{v\neq s}l(v)$ will be called a *diameter*.

In a homogeneous (e.g., regular) network and a weakly disordered network (e.g., SW network), all vertices are equivalent after an average over all disorder realizations. The diameter is independent of the source, $D_s=D$. In such cases we select the source s arbitrarily. On the other hand, the SF network has a highly inhomogeneous structure. For the SF network, we select the *hub* which has the largest degree as the source s since it plays the most important role in the transport [13].

The spanning tree $\mathbf{T}_s$ of a disordered network will be different from $\mathbf{T}_s^0$ of the same network without disorder. If the disorder has a continuous distribution, with probability 1, all shortest paths are uniquely determined. Therefore, $\mathbf{T}_s$ has a tree structure, whereas $\mathbf{T}_s^0$ may have loops. Without loops, $\mathbf{T}_s$ consists of only $(N-1)$ edges. Moreover, a vertex may have a shortest path that cannot be found in $\mathbf{T}_s^0$. For example, a path (s,v_1,v_9,v_8,v_6) in a network in Fig. 1 may be a shortest path to v_6, so that $\mathbf{T}_s$ includes the edge $[v_8;v_6]$ which does not belong to $\mathbf{T}_s^0$. Such an edge of $\mathbf{T}_s$ that does not belong to $\mathbf{T}_s^0$ will be called an *activated* edge. The disorder activates it to play a role in the transport. The activated edge results in a drastic change in the shape of the spanning tree and increases the network diameter. We quantify the change by the density of disorder-induced activated edges Φ, which is given by the number of activated edges in $\mathbf{T}_s$ divided by $(N-1)$, and the diameter-expansion coefficient $\Upsilon=(D_s-D_s^0)/D_s^0$ with D_s (D_s^0) the diameter with (without) disorder. The activated edge emerges as a result of competition between all paths connecting a vertex to the source. So networks with different structures respond differently. In the following section we will study the evolution of the spanning trees of the regular network and the small-world network [3].

III. SMALL-WORLD NETWORK

Consider a regular network consisting of N vertices on a one-dimensional ring, each of which is connected up to Zth nearest neighbors with undirected edges. The SW network is obtained by rewiring each edge with probability p_r (see Ref.
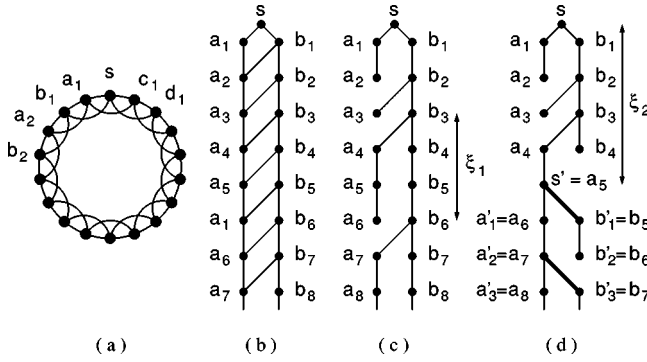
FIG. 2. A regular network with $Z=2$ in (a) and its spanning trees without disorder in (b) and with disorder in (c) and (d). (c) shows a spanning tree of type B and (d) shows a spanning tree with both segments of type A and type B. Vertices in (b), (c), and (d) are arranged in the hierarchical order in the separation from the source s. Activated edges are represented by thick lines in (d).

[3] for a detailed procedure). Except for extreme cases with $p_r=0$ (regular network) and $p_r=1$ (random network), the SW network displays the small-world phenomena [3]. We introduce a quenched disorder in edge costs as in Eq. (1) with the disorder distribution

$$\mathcal{F}(\eta) = \begin{cases} \dfrac{1}{2\varepsilon} & \text{for } -\varepsilon \le \eta < \varepsilon \\ 0 & \text{otherwise.} \end{cases} \tag{2}$$

Disorder strength is controlled by the parameter ε (<1). First we focus on the regular network ($p_r=0$) with $Z=2$, which gives us a lot of insights.

A. Regular network ($p_r=0$) with $Z=2$

A regular network with $Z=2$ and $N=18$ is shown in Fig. 2(a). We consider the shortest path from the source s. Without disorder ($\varepsilon=0$), the shortest path to b_n is unique. On the other hand, there are n degenerate shortest paths to a_n. So the spanning tree $\mathbf{T}_s^0$ has a ladder shape with diagonal rungs from b_n to a_{n+1} as shown in Fig. 2(b) [19]. All edges $\{[a_n;b_n]\}$ are missing in $\mathbf{T}_s^0$.

With infinitesimal disorder, all loops break up in the spanning tree. So either $[a_{n-1};a_n]$ or $[b_{n-1};a_n]$ should be removed from $\mathbf{T}_s$. Consequently, $\mathbf{T}_s$ has a tree shape with a single branch for b_n's and with sub-branches for a_n's, cf. Fig. 2(c). This shape will be denoted as a type-B tree. The branching points are determined from recursion relations for the distances $d(a_n)$ and $d(b_n)$,

$$d(a_n) = \min\{d(a_{n-1}) + c([a_{n-1};a_n]), \; d(b_{n-1})$$
$$+ c([b_{n-1};a_n])\}, \tag{3}$$

$$d(b_n) = d(b_{n-1}) + c([b_{n-1};b_n]). \tag{4}$$

If $d(a_{n-1}) + c([a_{n-1};a_n]) < d(b_{n-1}) + c([b_{n-1};a_n])$, the predecessor of a_n is a_{n-1}, otherwise the predecessor is b_{n-1}. The recursion relations (3) and (4) holds if $\mathbf{T}_s$ has the type-B structure, which is valid as long as

$$d(a_n) + c([a_n;b_n]) > d(b_n). \tag{5}$$

When it is violated, the predecessor of b_n is a_n, $[a_n;b_n]$ becomes activated, and $\mathbf{T}_s$ changes its shape.

We introduce now a random-walk interpretation of the recursion relation. Define $X_A(n) \equiv d(a_n) - n$ and $X_B \equiv d(b_n) - n$ and insert it into Eq. (4). Using Eq. (1), one obtains $X_B(n) = X_B(n-1) + \eta([b_{n-1};b_n])$; $X_B(n)$ can be interpreted as the coordinate of a one-dimensional random walker (walker B) after n jumps. $X_A(n)$ is given by the minimum of $X_A(n-1) + \eta([a_{n-1};a_n])$ and $X_B(n-1) + \eta([b_{n-1};a_n])$. The first term also suggests that $X_A(n)$ can be interpreted as the coordinate of another random walker (walker A) after n jumps. But its motion is constrained: After each jump, one has to compare the current position of A (the first term) with the position of B [the second term$\approx X_B(n) + O(\varepsilon)$], and take the minimum as $X_A(n)$. Therefore, one may assume a hard-core repulsion between two walkers [the interaction range fluctuates by an amount of $O(\varepsilon)$]. The inequality in Eq. (5) can be rewritten as $X_B(n) - X_A(n) < c([a_n;b_n]) = 1 + O(\varepsilon)$, which imposes a constraint on the random-walk motion.

It is convenient to introduce $X_R(n) \equiv X_B(n) - X_A(n)$. It can be interpreted as the coordinate of a one-dimensional random walker R in the presence of a fluctuating *reflecting* wall at $X_R = O(\varepsilon)$ and a fluctuating *absorbing* wall at $X_R = 1 + O(\varepsilon)$. At each time step, the walker R performs a jump of size η' obeying the distribution $\mathcal{F}_R(\eta') \equiv \int d\eta_1 \int d\eta_2 \mathcal{F}(\eta_1) \mathcal{F}(\eta_2) \delta(\eta' - \eta_1 + \eta_2)$. Hereafter, the boundary walls are assumed to be fixed at $X_R = 0$ and $X_R = 1$. The fluctuations do not modify the scaling behavior of Φ and Υ with a possible change in the coefficient of the leading order term.

The random walker R determines the shape of the spanning tree. If the walker does not touch either wall at $X_R = 0$ or 1 at a moment n, then the predecessor of a_n (b_n) is a_{n-1} (b_{n-1}). When it bounces at the reflecting wall in step n, a_n has b_{n-1} as its predecessor, and the spanning tree has a new sub-branch, cf. a_3, a_4, and a_7 in Fig. 2(c). If it collides with the absorbing wall at step n_0, the inequality (5) is violated and b_{n_0} has a_{n_0} as predecessor instead of b_{n_0-1} [see the spanning tree in Fig. 2(d) which has $n_0=5$].

The same random-walk mapping can be established after an edge $[a_{n_0};b_{n_0}]$ is activated. If one interprets $s' = a_{n_0}$ as a new source and redefines $a_n' = a_{n+n_0}$ and $b_n' = b_{n+n_0-1}$, the distances from s' to a_n' and b_n' satisfy the same recursion relation as in Eqs. (3) and (4) and the same constraint as in Eq. (5) with $a(b)$ replaced by b' (a'). Thus, the spanning tree consists of a single branch for a''s and sub-branches for b''s. This shape will be denoted as a type A, see Fig. 2(d). The creation of sub-branches and the switch into type-A tree are described by the same random-walk mapping used for the type-B segment.

Combining the mappings for type-A and type-B segments, the shape of the whole spanning tree can be determined by the the random walker R in the presence of two hard-core walls at $X_R=0$ and 1. Initially $X_R(0)=0$, and the wall at $X_R=0$ (1) is reflecting (absorbing). When the ab-

sorbing wall is at $X_R = 1$ (0), the spanning tree has the type-B (type-A) shape. The sub-branch emerges when the random walker collides with the reflecting wall. When it collides with the absorbing wall, the role of the two walls are exchanged and the spanning tree switches its shape. It is interesting to note that the random walks with two types of boundary walls were used to find the exact ground states of one-dimensional random-field Ising-spin chain [20].

The shape of $\mathbf{T}_s$ is characterized by two length scales ξ_1 and ξ_2, see Fig. 2. The former characterizes the length of the sub-branch, and the latter the length of each type-A or type-B segment. They are given by the mean time scales between successive collisions with the reflecting wall and the absorbing wall, respectively. Then, ξ_1 can be approximated as the lifetime of the random walker R, being at the origin initially, in the presence of two absorbing walls at $X = 0$ and $X = 1$. And ξ_2 is given by the mean lifetime of the random walker R, being at the origin initially, in the presence of two absorbing walls at $X = \pm 1$. The lifetime τ of a random walker in the presence of absorbing boundary walls has been studied in various literatures. Here, we use the result $\tau = W_R W_L / \sigma^2$ in Ref. [21] where W_R (W_L) is the distance from the right (left) boundary wall. Taking $W_L = \sigma$ and $W_R = 1 - \sigma$ for ξ_1 and $W_R = W_L = 1/2$ for ξ_2, and using $\sigma^2 \equiv \int d\eta' \, \mathcal{F}(\eta') \eta'^2 = \frac{2}{3}\varepsilon^2$, we obtain that $\xi_1 \simeq \sqrt{3/2}\,\varepsilon^{-1}$ and $\xi_2 = (3/2)\varepsilon^{-2}$. Note that the $O(\varepsilon)$ fluctuation of the walls does not change the scaling exponents, but may modify the coefficient of ξ_1.

One edge among Z edges in a row is activated when a sub-branch appears only in the type-A segment [see Fig. 2(d)]. So, the activated-edge density is inversely proportional to ξ_1,

$$\Phi_{REG}(\varepsilon) = \frac{1}{Z} \frac{Z-1}{Z} \xi_1^{-1} \simeq \frac{1}{\sqrt{24}} \varepsilon, \qquad (6)$$

where $Z = 2$ and $(Z-1)/Z$ is the fraction of the type-A segments. When the spanning tree changes its shape at a certain vertex [cf. a_5 in Fig. 2(d)], its all descendent vertices increase their separation from s by 1. So, the diameter-expansion coefficient is inversely proportional to ξ_2,

$$\Upsilon_{REG}(\varepsilon) = \frac{1}{Z}\xi_2^{-1} = \frac{1}{3}\varepsilon^2. \qquad (7)$$

The results are valid in the asymptotic limit where $N \gg \max(\xi_1, \xi_2) = \xi_2$, which suggests the finite-size-scaling form $\Phi_{REG}(\varepsilon, N) = N^{-1/2} \mathcal{G}_\Phi(\varepsilon N^{1/2})$ and $\Upsilon_{REG}(\varepsilon, N) = N^{-1} \mathcal{G}_\Upsilon(\varepsilon N^{1/2})$. The scaling functions behave as $\mathcal{G}_\Phi(x) \simeq \chi_\Phi x$ and $\mathcal{G}_\Upsilon(x) \simeq \chi_\Upsilon x^2$ for $x \gg 1$. The scaling behavior is confirmed numerically. We compute both quantities for the regular network with $Z = 2$ and $N = 10\,000, \ldots, 80\,000$, which were averaged over 200 samples. They are plotted in Fig. 3, where data collapse very well. From a least-squares fitting we obtained that $\chi_\Phi \simeq 0.24$ and $\chi_\Upsilon \simeq 0.32$, which is close to the analytic results (6) and (7).

The extension to the regular networks with $Z > 2$ is straightforward. Vertices are labeled as $(s, v_1^1, \ldots, v_1^Z, v_2^1, \ldots, v_2^Z, \ldots)$ starting from the source s. Then, without
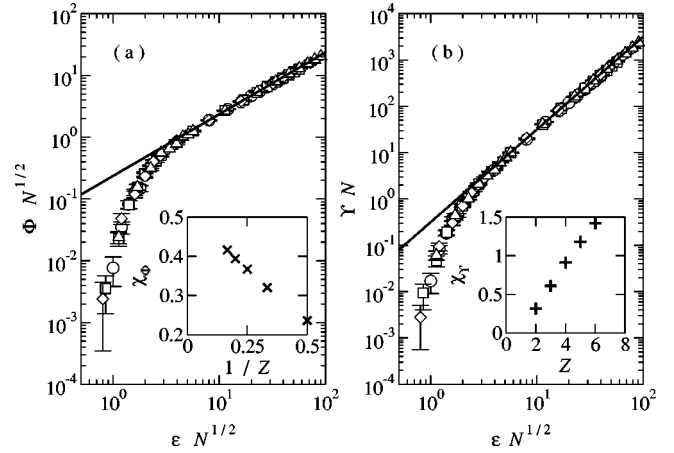
FIG. 3. Φ_{REG} in (a) and Υ_{REG} in (b) for the regular network with $Z = 2$ and $N = 10\,000$ ($\bigcirc$), $20\,000$ (), $40\,000$ ($\diamond$), and $80\,000$ ($\triangle$). The straight lines represent $0.24x$ in (a) and $0.32x^2$ in (b). Insets show Z dependence of the coefficients χ_Φ ($\Phi_{REG} \simeq \chi_\Phi \varepsilon$) and χ_Υ ($\Upsilon_{REG} \simeq \chi_\Upsilon \varepsilon^2$).

disorder, the spanning tree $\mathbf{T}_s^0$ has a Z-leg ladder structure with diagonal rungs. Each leg ($i = 1, \ldots, Z$) consists of vertices $\{v_n^i\}$. The predecessors of a node v_{n+1}^i are v_n^j with $j = i, \ldots, Z$. Edges $\{[v_n^i; v_n^j]\}$ with $i \neq j$ do not belong to $\mathbf{T}_s^0$. When the disorder turns on, there emerge activated edges. Until one finds an activated edge, the distance to each vertex from the source satisfies recursion relations

$$d(v_n^i) = \min_{j = i, \ldots, Z} \{d(v_{n-1}^j) + c([v_{n-1}^j; v_n^i])\}. \qquad (8)$$

The recursion relations are valid as long as

$$d(v_n^i) + c([v_n^i; v_n^j]) > d(v_n^j) \qquad (9)$$

for all $i \neq j$. With the mapping $X_i(n) = d(v_n^i) - n$, one can interpret $X_i(n)$ as a coordinate of a random walker A_i after n jumps [each jump has the distribution $\mathcal{F}(\eta)$]. Then, Eq. (8) implies a hard-core interaction between walkers, so A_i cannot overtake A_j's with $j > i$. Effectively, it suffices to consider the hard-core interaction only between A_i and A_{i+1}. If A_i and A_{i+1} collide at step n, then the vertex v_n^i takes v_{n-1}^{i+1} as its predecessor. Otherwise, v_{n-1}^i is the predecessor of v_n^i. The constraint (9) implies that the relative distance between all walkers should be less than $1 + O(\varepsilon)$, that is, $|X_1 - X_Z| \lesssim 1$. An activated edge $[a_{n_0}^1; a_{n_0}^Z]$ appears when this inequality is violated in the $(n_0 + 1)$th step. Then, we can use the same random-walk mapping after a cyclic permutation $(A_1, \ldots, A_Z) \to (A_2, \ldots, A_Z, A_1)$, which continues repeatedly. As in the case with $Z = 2$, the shape of the spanning tree is characterized by the length scale ξ_1, the mean time scale for a collision between adjacent walkers, and ξ_2, the mean time scale for violating the constraint $|X_1 - X_Z| \lesssim 1$. The time scales are approximately equal to those for the two-random-walker problem with a constraint $|X_1 - X_2| \lesssim 2/Z$. With this approximation, one gets $\xi_1 \sim (Z\varepsilon)^{-1}$ and $\xi_2 \sim (Z\varepsilon)^{-2}$. Using $\Phi_{REG} = (Z-1)/Z^2 \xi_1$ and $\Upsilon_{REG} = 1/Z\xi_2$, we finally obtain $\Phi_{REG} \simeq \chi_\Phi \varepsilon^1$ and $\Upsilon_{REG} \simeq \chi_\Upsilon \varepsilon^2$ with Z dependent coef-
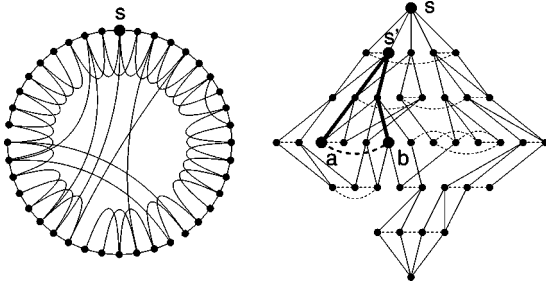
FIG. 4. A small-world network (left) with $N=40$, $Z=2$, and $p_r=0.1$ and its spanning tree $\mathbf{T}_s^0$ (right) without disorder. The dashed lines indicate edges which do not belong to $\mathbf{T}_s^0$.

ficients $\chi_\Phi \propto (1-1/Z)$ and $\chi_\Upsilon \propto Z$. The scaling exponents are universal for all Z. We determine the coefficients of ε and ε^2 for Φ_{REG} and Υ_{REG}, respectively, numerically and plot them as a function of Z in the insets of Fig. 3. One sees that $\chi_\Phi \propto (1-1/Z)$ and $\chi_\Upsilon \propto Z$, as estimated above.

We conclude that the quenched disorder is a relevant perturbation to the spanning tree of the regular network. Using the random-walk mapping, we have shown that a finite fraction of edges in the spanning tree are modified at nonzero disorder strength. This fraction is linearly proportional to the disorder strength, $\Phi_{REG} \sim \varepsilon$. We have also shown that the diameter-expansion coefficient is proportional to the square of the disorder strength, $\Upsilon_{REG} \sim \varepsilon^2$.

B. Small-world network

Next we study the effect of the quenched disorder in the SW network. Figure 4 shows an example of a SW network and its spanning tree $\mathbf{T}_s^0$ without disorder ($\varepsilon=0$). The random rewiring of edges randomizes $\mathbf{T}_s^0$, too, which is not suited for an exact description. Therefore we study Φ_{SW} and Υ_{SW} first numerically. We calculate Φ_{SW} in SW networks with $Z=4$ and $p_r=0.2$ and compare it with Φ_{REG} in Fig. 5. Φ_{SW} shows two noticeable features: (i) At small ε, Φ_{SW} appears to display a threshold behavior at a nonzero value of ε. (ii) Φ_{SW} has a strong size dependence. Φ_{SW} does not
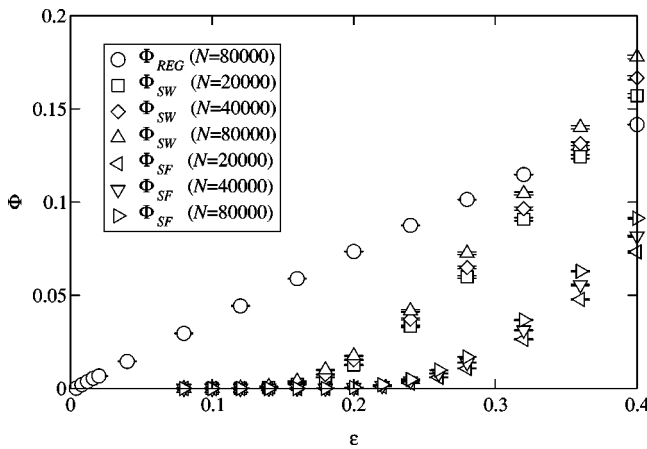
FIG. 5. Activated-edge densities in the regular network Φ_{REG} with $Z=4$, the SW network Φ_{SW} with $Z=4$ and $p_r=0.2$, and the SF network Φ_{SF} with $Z=Z_0=4$.

approach an asymptotic saturation at any value of ε and N considered. The same feature is commonly observed at other values of Z and p_r, and also for Υ_{SW}. In what follows we describe the response of the spanning tree with an effective random-walk process and we will show that the origin of the apparent threshold behavior is the presence of a well-defined ε-dependent crossover size in the network.

All edges that connect vertices at the same hierarchy level in $\mathbf{T}_s^0$, as represented by dashed lines in the example in Fig. 4, are candidates for an activated edge. Focus on a pair of vertices a and b with $[a;b] \notin \mathbf{T}_s^0$ in Fig. 4. They are descendants of a common ancestor s'. The edge $[a;b]$ belongs to $\mathbf{T}_s$ if a difference between costs of the two paths (denoted by thick lines) from s' to a and to b is larger than the edge cost $c([a;b])=1+\eta([a;b])=1+O(\varepsilon)$, where $O(\varepsilon)$ term can be neglected. The probability with which this happens will be denoted as $P_{act}([a;b])$. Let $l(a,b)$ be the separation of a and b to their common ancestor s' in $\mathbf{T}_s^0$. Using Eq. (1), the path costs are given by a sum of $l(a,b)$ independent random variables η's [plus $l(a,b)$]. So, with the common term $l(a,b)$ discarded, they can be interpreted as coordinates of two one-dimensional random walkers after $l(a,b)$ jumps. Each jump follows the distribution $\mathcal{F}(\eta)$. $P_{act}([a;b])$ is then given by the probability that the distance between two random walkers is larger than 1 after l jumps. Or equivalently, it is given by the probability that a random walker deviates from a starting position by a distance larger than 1 after l jumps, where each jump follows a distribution $\mathcal{F}_R(\eta')=\int d\eta_1 \int \eta_2 \mathcal{F}(\eta_1)\mathcal{F}(\eta_2)\delta(\eta'-\eta_1+\eta_2)$. The probability distribution of the random walker after l steps is given by $P_{RW}(x,l)=(2\pi\sigma^2 l)^{-1/2}e^{-x^2/(2\sigma^2 l)}$ with $\sigma^2 \equiv \int d\eta' \eta'^2 \mathcal{F}_R(\eta')=2\varepsilon^2/3$. Therefore, one obtains

$$P_{act}([a;b])=\mathrm{erfc}\left(\frac{\sqrt{3}}{2\varepsilon\sqrt{l(a,b)}}\right), \qquad (10)$$

where $\mathrm{erfc}(x) \equiv (2/\sqrt{\pi})\int_x^\infty e^{-x^2}$ is the complementary error function.

Now we make a mean-field-type approximation that each edge $e \notin \mathrm{T}_s^0$ may be an activated edge independently. That is only true for the edges $\{e_i=[a_i;b_i] \notin \mathbf{T}_s^0\}$ if the paths from a_i and b_i to their common ancestor do not overlap for different e_i's. Otherwise, two probabilities $P_{act}(e)$ and $P_{act}(e')$ are not independent. If e is activated, it modifies the shape of the spanning tree and hence $P_{act}(e')$, and vice versa. The approximation would give the correct scaling behavior if the spanning tree would be random and self-averaging. In the mean-field scheme, the activated-edge density is proportional to the probability in Eq. (10) with $l(a,b)$ replaced by the average value, i.e., the diameter of the network $D_s \sim \ln N$ [22],

$$\Phi_{SW}(N,\varepsilon) \simeq \alpha_1 \mathrm{erfc}\left(\frac{\alpha_2}{\varepsilon\sqrt{\ln N}}\right) \qquad (11)$$

with constants $\alpha_{1,2}$ being independent of ε and N.
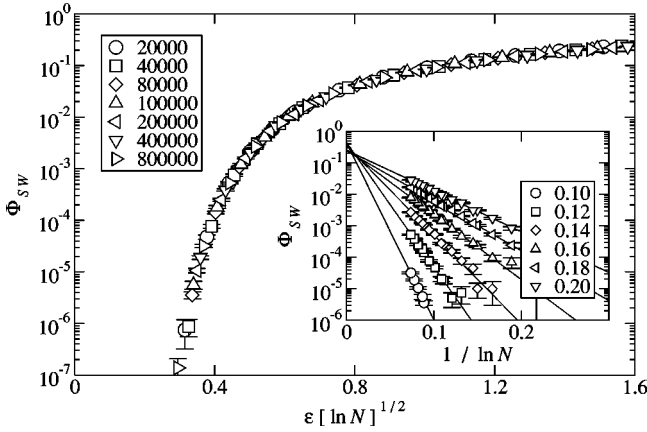
FIG. 6. Scaling plot of Φ_{SW} vs $\varepsilon(\ln N)^{1/2}$ according to Eq. (11). The inset shows that $\ln \Phi \simeq a + b/\ln N$ for fixed values of ε, following Eq. (12). The straight lines are obtained from a least-square fitting.

FIG. 7. Scaling plot of Φ_{SF} vs $\varepsilon(\ln N/\ln\ln N)^{1/2}$ for the Barabási-Albert networks with $Z = Z_0 = 2$ and $N = 20\,000, \dots, 80\,0000$. Inset shows a plot of Φ_{SF} vs $1/(\varepsilon^2[\ln N/\ln\ln N])$ in semilog scale.

The scaling function behaves as $\mathrm{erfc}(x) \simeq 1 - (2/\sqrt{\pi})x$ for small x. So, in the asymptotic limit where $N \gg N_c \simeq e^{\alpha_2^2 \varepsilon^{-2}}$, the activated-edge density is a constant ($\Phi_{SW} \simeq \alpha_1$) in the infinite ($N \to \infty$) network for all values of $\varepsilon \neq 0$. Therefore, the spanning tree of the SW network undergoes a discontinuous transition at $\varepsilon = \varepsilon_c = 0$ in the asymptotic limit, which is contrasted to the continuous transition in the regular network.

The asymptotic behavior sets in when the network size is bigger than the crossover size $N_c \simeq e^{-\alpha_2^2 \varepsilon^{-2}}$. It grows very fast as ε goes to zero. For instance, when $\varepsilon = 0.1$ with $\alpha_2 \simeq 1$, only SW networks with $N \gg N_c \simeq 10^{43}$ are in the asymptotic region, which is improbable in any real networks. So, the behavior in the nonasymptotic regime is more important in practice. Using $\mathrm{erfc}(x) \simeq (1/\sqrt{\pi}x)e^{-x^2}$ for $x \gg 1$, we obtain that

$$\Phi_{SW} \simeq \frac{\alpha_1 \varepsilon \sqrt{\ln N}}{\alpha_2 \sqrt{\pi}} \exp\left[-\frac{\alpha_2^2}{\varepsilon^2 \ln N} \right] \qquad (12)$$

for $N \ll N_c$. It has an essential singularity at $\varepsilon = 0$ and increases continuously and extremely slowly. Therefore, the spanning tree of finite SW networks undergoes an infinite-order transition at $\varepsilon = 0$.

Numerical data are in good agreement with the mean-field results. In Fig. 6, we plot Φ_{SW} as a function of the scaling variable $\varepsilon \sqrt{\ln N}$. Data at different values of N collapse onto a single curve, which supports the scaling form in Eq. (11). In the inset, we plot Φ_{SW} at given values of ε against $1/\ln N$ for $N = 100, \dots, 80\,0000$ in the semilog scale. We observe that the data align along straight lines, which support the result in Eq. (12). Extrapolating the straight lines to the limit $\ln N \to \infty$, we obtained that Φ_{SW}'s converge to $\alpha_1 \simeq 0.25$.

In the regular network, an activated edge may or may not increase the separation of vertices from the source, which leads to the different scaling behaviors of $\Phi_{REG} \sim \varepsilon$ and $\Upsilon_{REG} \sim \varepsilon^2$. However, in the SW network, all activated edges

considered above increase the separation. So Υ_{SW} shows the same scaling behavior as Φ_{SW}, which we also confirmed numerically.

IV. BARABÁSI-ALBERT SCALE-FREE NETWORK

In this section we study the response of the spanning tree of a SF network to the quenched disorder. We consider the Barabási-Albert (BA) network with the degree-distribution exponent $\gamma = 3$ [4]. Among all vertices, the hub which has the largest degree plays an important role in the SF network [13]. So we consider the spanning tree of the BA network with the hub as the source. Φ_{SF} is measured for the BA network with $Z_0 = Z = 4$, and compared with Φ_{REG} and Φ_{SW} in Fig. 5. Φ_{SF} behaves similarly to Φ_{SW}.

Though the SF network is different from the SW network in many aspects, its spanning tree also has a random structure. Thus, we expect that the scaling behavior of Φ_{SF} can be explained with the same mean-field-type approximation as Φ_{SW}. Under the approximation, each edge that does not belong to $\mathbf{T}_s^0$ may be activated independently. Then, the mean density of the activated edges is obtained by replacing $l(a,b)$ in Eq. (10) with the diameter of the network. Recently, it was found that the scale-free network is ultrasmall in diameter [23]. In particular, for $\gamma = 3$ (γ: the degree-distribution exponent) the diameter scales as $D \sim \ln N/\ln\ln N$, i.e., with a double-logarithmic correction to the SW scaling $D \sim \ln N$. It leads us to conclude that

$$\Phi_{SF} = \alpha_1' \mathrm{erfc}\left(\frac{\alpha_2'}{\varepsilon \sqrt{\ln N/\ln\ln N}} \right) \qquad (13)$$

with constants α_1' and α_2'.

This scaling form is indeed supported by our numerical data. In Fig. 7, we plot Φ_{SF} for the BA network with $Z = Z_0 = 2$ as a function of the scaling variable $\varepsilon \sqrt{\ln N/\ln\ln N}$, and obtain a good data collapse. Though the double-logarithmic correction is very weak, the data do not collapse at all without it. We note that the data also scale well with a

scaling variable $\varepsilon(\ln N)^{1/4}$, however, we presume that this is accidental since the ratio between $(\ln N/\ln \ln N)$ and $(\ln N)^{1/2}$ remains almost constant up to $N = 80\,0000$. The inset in Fig. 7 shows that $\ln \Phi_{SF}$ is linear in $1/(\varepsilon^2 \ln N/\ln \ln N)$. It implies that the scaling function has the essential singularity as in Eq. (12). The same scaling behavior is observed universally for other values of $Z=Z_0=3$ and 4, and also for Υ_{SF}.

The SF network shares the same scaling behavior with the SW network with the scaling variable $\varepsilon(\ln N/\ln \ln N)^{1/2}$. The spanning tree of the SF network undergoes a discontinuous transition in the asymptotic regime: Φ_{SF} and Υ_{SF} in the infinite SF networks jump from zero at $\varepsilon = 0$ to finite values as the disorder turns on. The asymptotic behavior sets in only when $N \gg N_c \sim \exp(\alpha|\ln \varepsilon|\varepsilon^{-2})$ with a positive constant α. In the transient regime with $N \ll N_c$, the spanning tree of the SF networks undergoes a continuous infinite-order transition with the essential singularity in Φ_{SF} and Υ_{SF} at $\varepsilon = 0$. Note that the crossover size N_c of the SF network grows much faster than that of the SW network. Therefore, we conclude that the scale-free network has the most stable transport pattern.

V. CONCLUSION

In a network the shortest paths between vertices play an important role. The optimal transport pattern from or to a vertex s is characterized by the spanning tree $\mathbf{T}_s$, a set of all shortest paths. We have investigated the response of the spanning tree of complex networks to a quenched randomness in edge costs, and found that the quenched disorder is a relevant perturbation. As the disorder turns on, the spanning tree evolves with a finite fraction of edges modified and the network diameter expands.

For the regular network, the shape of the spanning tree can be described exactly using the random-walk mapping. The spanning tree undergoes a continuous transition with $\Phi_{REG} \sim \varepsilon$ and $\Upsilon_{REG} \sim \varepsilon^2$ with ε the disorder strength. For the SW and SF networks, we obtain the scaling form $\Phi(\varepsilon, N) = \tilde{\Phi}(\varepsilon D^{1/2})$ where D is the network diameter. It scales as $D \sim \ln N$ in the SW network and $D \sim \ln N/\ln \ln N$ in the BA network [23]. The diameter-expansion coefficient satisfies the same scaling form. The scaling function approaches a constant as its argument $x = \varepsilon D^{1/2} \to \infty$. It has the essential singularity, $\tilde{\Phi}(x) \sim \exp(-\alpha x^{-2})$ with a positive constant α, as $x \to 0$. Therefore, Φ and Υ have a *discontinuous* jump at $\varepsilon = 0$ in infinite-size SW and SF networks. It shows that the SW network and the SF network are more affected by the

quenched disorder than the regular network. However, the asymptotic scaling behavior emerges only when the network size is larger than the crossover size N_c. It grows as $N_c \sim \exp(\alpha \varepsilon^{-2})$ for the SW network and $N_c \sim \exp(\alpha|\ln \varepsilon|\varepsilon^{-2})$ for the BA network with a positive constant α as ε vanishes. Since the crossover size grows extremely fast as ε goes to zero, the behavior in the transient regime with $N \ll N_c$ is more important in practice. In contrast to the discontinuous jump when $N \gg N_c$, Φ at $N \ll N_c$ grows continuously and very slowly with the essential singularity at $\varepsilon = 0$. Numerically we obtained that $\Phi < 10^{-7}$ for $\varepsilon \lesssim 0.1$ up to $N = 800\,000$. Therefore, we conclude that the transport pattern in finite SW and SF networks is extremely robust against the quenched disorder. In particular, the SF network is most stable.

The interesting scaling behavior of the SW and SF networks can be explained within a mean-field picture. Φ and Υ are proportional to the probability that a displacement of a random walker with diffusion constant $O(\varepsilon^2)$ is larger than 1 after D, the network diameter, time steps. The crossover size is determined from the condition $\varepsilon^2 D(N_c) \simeq 1$, and the spanning tree is very stable against the disorder as long as $N \ll N_c$. So, the exponential divergence of the crossover size N_c and hence the extreme stability of the spanning tree are the direct consequence of the small worldness, i.e., $D(N) \sim \ln N$ [22] and $D(N) \sim \ln N/\ln \ln N$ [23], for the small-world and the scale-free network, respectively. The diameter of the SF networks with $2 < \gamma < 3$ scales as $D(N) \sim \ln \ln N$ [23] and within the mean-field picture one expects the crossover size of these networks to scale like $N_c \sim \exp[\exp(-\alpha \varepsilon^{-2})]$.

Another consequence of the disorder is that the shortest path from one vertex to the other becomes unique. Recently, it has been reported that the load distribution in SF networks follows a power-law distribution with the universal load-distribution exponent $\eta \simeq 2.2$ or 2.0 [13,16]. Phenomenologically, the SF networks with degenerate shortest paths seem to have $\eta \simeq 2.2$ [13,16], whereas those without or only a few degenerate shortest paths seem to have $\eta \simeq 2.0$ [14,16]. It would be interesting to study the load distribution in the disordered SF networks, which will shed light on the role of the degeneracy on the universality of the load distribution. This work is in progress.

[1] S.H. Strogatz, Nature (London) **410**, 268 (2001).

[2] R. Albert and A.-L. Barabási, Rev. Mod. Phys. **74**, 47 (2002).

[3] D.J. Watts and S.H. Strogatz, Nature (London) **393**, 440 (1998).

[4] A.-L. Barabási and R. Albert, Science **286**, 509 (1999).

[5] A.-L. Barabási, R. Albert, and H. Jeong, Physica A **272**, 173 (1999); P.L. Krapivsky, S. Redner, and F. Leyvraz, Phys. Rev. Lett. **85**, 4629 (2000); S.N. Dorogovtsev, J.F.F. Mendes, and A.N. Samukhin, *ibid.* **85**, 4633 (2000).

[6] S.N. Dorogovtsev, A.V. Goltsev, and J.F.F. Mendes, Phys. Rev. E **66**, 016104 (2002).

[7] F. Iglói and L. Turban, Phys. Rev. E **66**, 036140 (2002).

[8] B.J. Kim, H. Hong, P. Holme, G.S. Jeon, P. Minnhagen, and M.Y. Choi, Phys. Rev. E **64**, 056135 (2001).

[9] R. Pastor-Satorras and A. Vespignani, Phys. Rev. Lett. **86**, 3200 (2001).

[10] R. Albert, H. Jeong, and A.-L. Barabási, Nature (London) **406**, 378 (2000).

[11] R. Cohen, K. Erez, D. ben-Avraham, and S. Havlin, Phys. Rev. Lett. **85**, 4626 (2000).

[12] D.S. Callaway, M.E.J. Newman, S.H. Strogatz, and D.J. Watts, Phys. Rev. Lett. **85**, 5468 (2000).

[13] K.-I. Goh, B. Kahng, and D. Kim, Phys. Rev. Lett. **87**, 278701 (2001).

[14] G. Szabó, M. Alava, and J. Kertész, Phys. Rev. E **66**, 026101 (2002).

[15] M.E.J. Newman, Phys. Rev. E **64**, 016131 (2001); **64**, 016132 (2001).

[16] K.-I. Goh, E.S. Oh, H. Jeong, B. Kahng, and D. Kim, Proc. Natl. Acad. Sci. U.S.A. **99**, 12583 (2002).

[17] M. Alava, P.M. Duxbury, C. Moukarzel, and H. Rieger, in *Phase Transitions and Critical Phenomena,* edited by C. Domb and J. L. Lebowitz (Academic Press, Cambridge, 2000), Vol. 18 pp. 141–317; A. Hartmann and H. Rieger, *Optimization Algorithms in Physics* (Wiley-VCH, Berlin, 2002).

[18] S.H. Yook, H. Jeong, A.-L. Barabási, and Y. Tu, Phys. Rev. Lett. **86**, 5835 (2001).

[19] The spanning tree has another ladder for vertices and c_n and d_n. At small disorder, the two branches evolve independently and do not overlap. So it suffices to consider only the single branch for a_n and b_n.

[20] G. Schröder, T. Knetter, M. Alava, and H. Rieger, Eur. Phys. J. B **24**, 101 (2001).

[21] R.D. Hughes, *Random Walks and Random Environments, Random Walks* (Clarendon, Oxford, 1995), Vol. 1.

[22] M.E.J. Newman, C. Moore, and D.J. Watts, Phys. Rev. Lett. **84**, 3201 (2000).

[23] R. Cohen and S. Havlin, e-print cond-mat/0205476.